SURFACE DESCRIPTION FOR CORNEA TOPOGRAPHY USING MODIFIED CHEBYSHEV-POLYNOMIALS

Alexandros Soumelidis [*,1] **Zoltán Fazekas** [*,1]
Ferenc Schipp [**,1,2] **János Németh** [***,1]

[*] *Systems and Control Laboratory, Computer and Automation Research Institute, Budapest, Hungary*
[**] *Department of Numerical Analysis, Eötvös Loránd University, Budapest, Hungary*
[***] *1st Department of Ophthalmology, Semmelweis University, Budapest, Hungary*

Abstract: The optical behaviour of the (human) cornea is often characterized with the Zernike-coefficients derived via the Zernike-transform of its optical power map. In this paper, a radial transform based on the Chebyshev-polynomials of the second kind is suggested for a surface-based, rather than an optical power map based representation of the cornea. This transform is well-suited for providing compact representations for quasi-hemispherical surfaces, and after appropriate argument-transform applied to these polynomials also for spherical-calotte-like surfaces. Examples illustrating the effect of the argument-transformation are also included in the paper.

Keywords: Biomedical systems, function approximation, radial base function, shape description, medical applications

1. INTRODUCTION

Cornea topographs are widely used in ophthalmologic diagnostics for video-keratoscopic examinations of patients. The purpose of such an examination is to determine and display the shape and/or the optical power of the living cornea. The cornea surface and the optical power of the cornea are normally displayed as a map (Corbett *et al.*, 1999). Such a map indicates either the actual height of the cornea surface, or, in case of an optical power map, the actual optical power at the particular cornea location. The map is then closely inspected by an ophthalmologist.

From this optical power map, optical aberration-features (e.g., astigmatism, coma) of the cornea are calculated by the cornea topograph. The ophthalmologist then evaluates the optical aberrations of the cornea, and using this and other information - e.g., the optical aberration of the whole eye measured with a Shack-Hartmann wavefront sensor - she chooses an appropriate treatment for the patient. For example, decides whether a sight-correcting laser operation of the eye would be beneficial for the patient, or not. With such operations the cornea is reshaped, and as an effect its optical surface and optical power is modified. Clearly, the precise knowledge of and the

[1] The authors gratefully acknowledge the support from the National Office for Research and Technology, Hungary, provided under Ref. number NKFP-2/020/04.
[2] The author gratefully acknowledges the support from the Hungarian Scientific Research Fund provided under Ref. numbers T047128 and T047132.

appropriate representation of the surface data is essential for the success of the operation.

Precise and quick representation of the corneal surface is also very important for the investigation of the tear-film behaviour (Németh *et al.*, 2002). In this paper, a radial orthogonal transformation that has promising features to generate concise representation of hemisphere-like surfaces is presented. This surface-based representation approach provides an alternative to the Zernike-based representation.

In Section 2, a radial orthogonal transformation that has the potential of producing a concise representation of hemisphere-like surfaces is chosen and described. In Section 3, an argument-transformation-based approach is presented that modifies the chosen orthogonal transformation, so that its application to calotte-like surfaces - such as the surface of a human cornea - will result in concise representation of such surfaces. In Section 4, some of the radial basis functions of the transformations and their modified versions for calotte-like surfaces are discussed. In Section 5, the future work with respect to the application of these transformations to cornea representations is outlined.

2. MATHEMATICAL MODELLING OF HEMISPHERE-LIKE SURFACES

A surface - e.g., a corneal surface - can be described by a two-variable function f(x,y). The application of the polar transform to variables x and y results in

$$x = r\cos\varphi, \quad y = r\sin\varphi, \tag{1}$$

where r and φ are the radial and the azimuthal variables, respectively, over the unit disk, i.e., where

$$0 \le r \le 1, \quad 0 \le \varphi \le 2\pi.$$

Using r and φ, f(x,y) can be transcribed in the following form:

$$F(r,\varphi) := f(r\cos\varphi, r\sin\varphi) \tag{2}$$

Function F is often expressed in Zernike-basis (Iskander *et al.*, 2001; Iskander *et al.*, 2002). The Zernike-basis is derived from the Zernike-polynomials in the following manner

$$Z_n^m(r,\varphi) := R_n^m(r)e^{im\varphi}, \tag{3}$$

where $0 \le |m| \le n$ and $m \in \mathbb{Z}$ and $n \in \mathbb{N}$. The Zernike-function Z_2^4 is shown in Fig. 1 as an illustration.

The system of Zernike-functions is orthogonal over the unit-circle with respect to the measure $r\,dr\,d\varphi$, that is

$$\int_0^1\int_0^{2\pi} Z_n^m(r,\varphi)\overline{Z}_{n'}^{m'}(r,\varphi)r\,drd\varphi = \frac{\pi}{n+1}\delta_{nn'}\delta_{mm'},$$

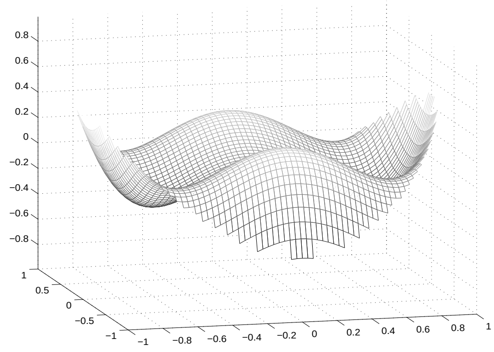

Fig. 1. The Zernike-function Z_2^4

where $\delta_{nn'}$ is the Kronecker-symbol.

It is of interest to note that the Zernike-polynomials R_n^m can be expressed by the Jacobi-polynomials $P_k^{\alpha,\beta}$:

$$R_n^m(r) = (-1)^{(n-m)/2}r^m P_{(n-m)/2}^{m,0}(1-2r^2).$$

With an eye on the efficient representation of real cornea surfaces, an alternative to the Zernike-system firstly for hemisphere-like surfaces is proposed. This system is based upon another well-known orthogonal system of functions, namely, the Chebyshev-polynomials of 2nd kind. The Chebyshev-polynomials of 2nd kind belong to the class of the Jacobi-polynomials with parameters $\alpha = 1/2$ and $\beta = 1/2$, see e.g. (Szegö, 1981).

The reasons for selecting these functions based on Chebyshev-polynomials are manifold. Firstly, the Chebyshev-polynomials are closely connected to the trigonometric system – an argument transform leads from the one to the other - and hence many of the methods and algorithms that are readily available for the trigonometric system are expected to work well also with the new system. Secondly, the application of the summation methods frequently used in conjunction with the trigonometric systems results in approximations that are uniformly convergent (i.e. convergent in C^1 norm) over the unit circle. Thirdly, the polynomials of the Chebyshev-system are orthogonal with respect to the weight function $\sqrt{1-r^2}$ $(0 \le r \le 1)$. As a consequence, the function $F(r,\varphi) = \sqrt{1-r^2}$, which describes a hemisphere (see Fig. 2), can be represented using the proposed system and its weight function as a single component.

This is of great significance for the mentioned application area, as the ideal cornea surface is often modelled as a spherical surface, i.e. its representation is very concise.

The Chebyshev-polynomials of 2nd kind can be introduced as follows: it can simply be proved, that $\sin nt/\sin t$ can be expressed as the polynomial of degree $n-1$ of $\cos t$, i.e.

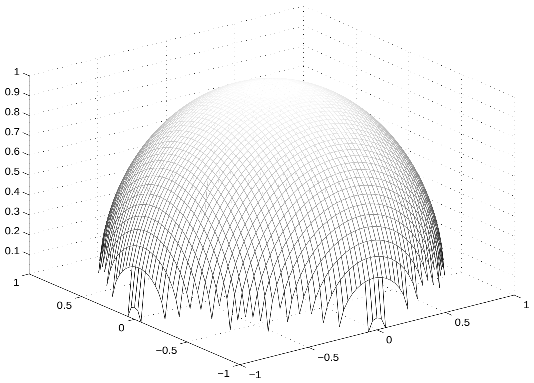

Fig. 2. The hemisphere over the unit circle

$$\frac{\sin nt}{\sin t} = U_n(\cos t) \quad (t \in \mathbb{R}, n \in \mathbb{N}). \tag{4}$$

The Chebyshev-polynomials of second kind satisfy the following second order recursion

$$\begin{aligned} U_1(x) = 1, \quad U_2(x) = 2x, \\ U_{n+1}(x) = 2xU_n(x) - U_{n-1}(x) \\ (x \in \mathbb{R}, n = 1, 2, \cdots). \end{aligned} \tag{5}$$

Since functions U_n are even and odd for odd and even index values $n \in \mathbb{N}$, respectively, both the system of even functions, namely $V_n := U_{2n-1}$, and the system of odd functions, namely $W_n := U_{2n}$ are orthogonal over the interval $[0, 1]$, i.e. the following orthogonality relations can be expressed:

$$\int_0^1 V_n(r)V_m(r)\sqrt{1-r^2}\,dr = \frac{\pi}{4}\delta_{mn} \tag{6}$$

$$\int_0^1 W_n(r)W_m(r)\sqrt{1-r^2}\,dr = \frac{\pi}{4}\delta_{mn}. \tag{7}$$

In the rest of the paper, only the V_n system will be considered. Building upon the V_n system, let the following system of complex valued functions of variables r and ϕ be introduced:

$$\begin{aligned} \mathcal{V}_{nm}(r, \varphi) := V_n(r)e^{im\varphi} \\ ((r, \varphi) \in I,\ n \in \mathbb{N}, m \in \mathbb{Z}) \end{aligned} \tag{8}$$

This system – according to the orthogonality of the trigonometrical system – forms a complete orthogonal system in the unit disk $\mathbb{D} := \{(x, y) : x^2 + y^2 \leqq 1\}$ with respect to the weight-function $\rho(r, \phi) = \sqrt{1-r^2}$, where $((r, \phi) \in I := [0, 1] \times [0, 2\pi])$, i.e.

$$\int_0^1\int_0^{2\pi}\mathcal{V}_{nm}(r,\varphi)\overline{\mathcal{V}_{n'm'}(r,\varphi)}\rho(r,\varphi)d\varphi dr = \frac{\pi^2}{2}\delta_{mm'}\delta_{nn'}$$

$$((m, n), (m', n') \in \mathcal{N} := \mathbb{N} \times \mathbb{Z}). \tag{9}$$

The systems $\mathcal{V}_{nm}$ and $\mathcal{V}_{nm}\rho$ $((n, m) \in \mathcal{N})$ can be interpreted as a bi-orthogonal system in $L^2(I)$, with respect to the inner product

$$\langle f, g\rangle := \int_0^1 \int_0^{2\pi} f(r, \varphi)\overline{g(r, \varphi)}\,\rho(r, \varphi)\,d\varphi\,dr$$

Hence any function $F \in L^2(I)$ can be realized by

$$F \sim \sum_{(n,m)\in\mathcal{N}} \langle F, \mathcal{V}_{nm}\rangle \mathcal{V}_{nm}\rho \tag{10}$$

bi-orthogonal representation.

Specifically, if $F(r, \phi) := \sqrt{1-r^2}$ – i.e. a hemisphere surface, as shown in Fig. 2 – the representation will be reduced to a single component.

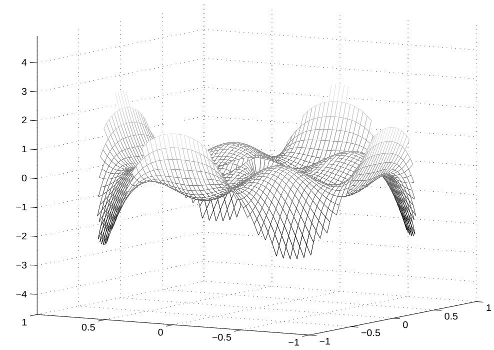

Fig. 3. The Chebyshev function $\mathcal{V}_3^4$

The representation (10) forms the basis of computation algorithms. All the practical numerical algorithms for computing the coefficients of a representation require some sort of discretization. Efficient algorithms can be obtained by choosing appropriate discretization. Let the following system of discrete points for the discretization of system V_n be introduced:

$$I_{NM} := \{(r_k^N, \varphi_\ell^M) : 1 \leq k \leq N, 0 \leq \ell < M\}$$

where

$$r_k^N := \cos\frac{k\pi}{2N+1} \quad (k = 1, 2, \cdots, N) \tag{11}$$

$$\varphi_\ell^M := 2\pi\ell/M \quad (\ell = 0, 1, \cdots, M-1), \tag{12}$$

r_k^N points are placed according to the positive roots of the polynomial V_N. It can easily be shown, that the system V_n system is orthogonal with respect to the discrete inner-product

$$[f, g]_N := \sum_{k=1}^N f(r_k^N)\overline{g(r_k^N)}(1 - |r_k^N|^2). \tag{13}$$

This orthogonality relation forms the basis for applying fast computational algorithms, e.g. FFT, for the approximate computing the coefficients of the surface representation.

3. THE ARGUMENT TRANSFORM

Argument transforms are widely used for generating new systems for ones already known. Many well-known orthogonal systems can be derived from the trigonometric system using various argument transforms. The Chebyshev-polynomials of the first and second kind, for example, are derived from the $\cos nx, \sin nx/\sin x$ trigonometric systems, respectively, using the $x = \arccos x$ argument transform.

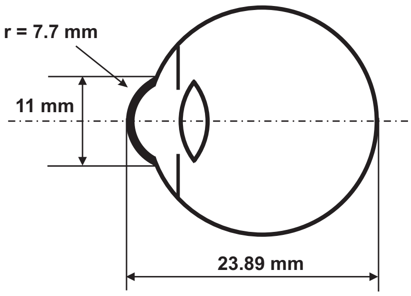

Fig. 4. Cornea on Gullstrand eye-model

The convenience of the argument transform applied to a trigonometric system has been demonstrated also in the field of signals and systems theory by (Soumelidis *et al.*, 2002). A noteworthy example for the use of argument transform in the given context is the generation of the discrete Laguerre-system from the e^{inx} complex trigonometric system. This exquisite origin of the Laguerre-system turns out to be very advantageous in several respects; e.g., in the computing of the Fourier-coefficients, or in the creation of discrete orthogonal systems.

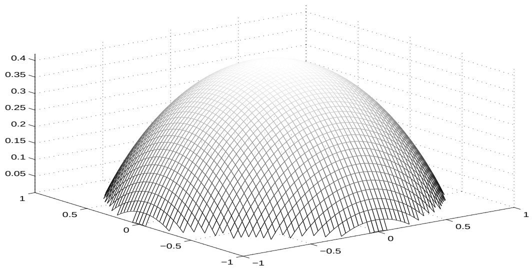

Fig. 5. A cornea-like "calotte" surface

Using the approach of argument transform described below, various useful orthogonal systems can be built from the $V_n(r)$ functions. The functions generated in this manner are orthogonal with respect to a non-negative weight function $\rho(t)$ $(0 \le t \le 1)$. The actual weight function can be chosen to match the requirements of the given application. E.g., when dealing with cornea surfaces - that is, surfaces assumed to be spherical calotte-like surfaces according to the relative simple Gullstrand eye-model shown in Fig. 4 – the proper choice for the weight function could be a circular segment rather than a semi-circle. In this case, the weight function $\sqrt{1-r^2}$ – which is used together with the original $V_n(r)$ functions – is replaced by

$$\varphi_a(r) := \sqrt{a^2 - r^2} - \sqrt{a^2 - 1} \qquad (0 \le r \le 1, a \ge 1). \tag{14}$$

For the standard cornea dimensions shown in Fig. 1, the value of parameter a is 1.4.

Applying the continuously differentiable bijection $R : [0, 1] \to [0, 1]$ on function $V_n(r)$ and using the argument transform $r = R(t)$ for (6), results in

$$\frac{\pi}{4}\delta_{mn} = \int_0^1 V_m(r)V_n(r)\sqrt{1-r^2}\,dr = \\ = \int_0^1 V_m(R(t))V_n(R(t))R'(t)\sqrt{1-R(t)^2}\,dt$$

Let the function R together with an appropriate constant c - be chosen in the following manner:

$$R'(t)\sqrt{1-R^2(t)} = c\rho(t) \quad (0 \le t \le 1) \tag{15}$$

where $\rho(t)$ is the required weight function for a particular application. This choice of function R results in a non-linear differential equation. In order to solve this differential equation, consider that the left-hand-side of this differential equation can be re-written as $d\Phi(R(t))/dt$, where

$$\Phi'(x) = \sqrt{1-x^2} \quad (-1 \le x \le 1) \tag{16}$$
$$\Phi(x) = \frac{x}{2}\sqrt{1-x^2} + \frac{1}{2}\arcsin x.$$

With the mentioned transcription, the above differential equation takes the following form:

$$\frac{d}{dt}\Phi(R(t)) = c\rho(t) \tag{17}$$

Integrating both sides of the equation according to variable t, and taking into consideration that $R(0) = 0$ and $R(1) = 1$,

$$\Phi(R(r)) = c\int_0^r \rho(t)\,dt \quad (0 \le r \le 1) \tag{18}$$

is obtained, while for constant c

$$c = \frac{\Phi(1)}{\int_0^1 \rho(t)\,dt} = \frac{\pi}{4\int_0^1 \rho(t)\,dt}. \tag{19}$$

Using these results, the sought argument transform is as follows.

$$R(r) = \Phi^{-1}\Big(c\int_0^r \rho(t)\,dt\Big) \quad (0 \le r \le 1), \tag{20}$$

where Φ^{-1} is the inverse function of Φ. Practically, by this train of thought the following theorem has been proved:

Theorem 1. Let $\rho(r)$ $(r \in [0, 1])$ be a continuous non-negative function, starting from the Chebyshev-polynomials of 2nd kind $V_n := U_{2n-1}$ by applying the argument-transform defined by (19) and (20) let the function

$$Y_n^\rho(r) := V_n(R(r)) \quad (n \in \mathbb{N},\ 0 \le r \le 1), \tag{21}$$

be introduced. In this case, the following orthogonality relation holds:

$$\int_0^1 Y_n^\rho(r)Y_m^\rho(r)\,\rho(r)\,dr = c_\rho\delta_{mn} \tag{22}$$

where

$$c_\rho := \int_0^1 \rho(t)\,dt, \quad m, n \in \mathbb{N}).$$

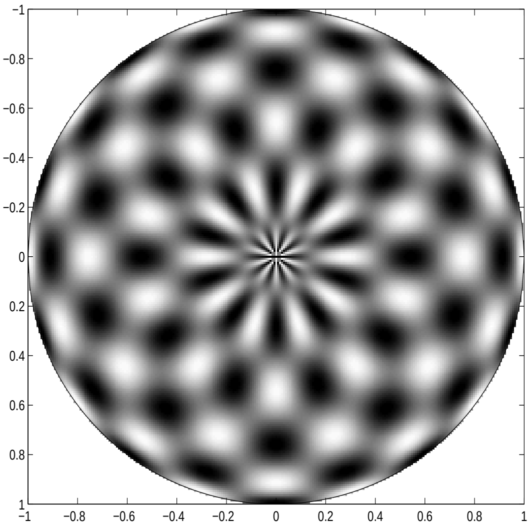

Fig. 6. The Chebyshev function $\mathcal{V}_{6,10}$

A discrete form of the orthogonality relation (22) also stands:

$$[f, g]_{\rho,N} := \sum_{t \in T_N^\rho} f(t)\overline{g(t)}(1 - R^2(t)) \qquad (23)$$

for T_N^ρ system of the discrete measurement points formed by applying R^{-1} to the radial values r_k^N of (11), while discretization on the azimuthal variable φ can the same as in (12).

4. MODELLING OF CALOTTE-LIKE SURFACES

As shown in Fig. 4, the Gullstrand eye-model describes the corneal surface as a spherical calotte. One can use the argument transform approach – described in detail in Section 3 for any arbitrary non-negative weight function - for the weight function $\varphi_a(r)$ (defined in (14). For this particular weight function – i.e., calculating (18) and (19) with $\rho(t) := \varphi_a(t)$ – the argument transform shown in Figure 8 is obtained.

The argument transform shifts the Chebyshev-polynomials and their roots in a non-linear fashion determined by the argument transform function. Figure 9 indicates how this argument transform tunes a particular Chebyshev-polynomial. The effect is also visible, if the grayscale plots of the original function $\mathcal{V}_{6,10}$ and of the modified function $\widehat{\mathcal{V}}_{6,10}$ in Figures 6 and 7, respectively, are compared.

Looking closely at the functions of the proposed system (e.g., at the function represented in Figure 6), and also those of the modified system (e.g.,

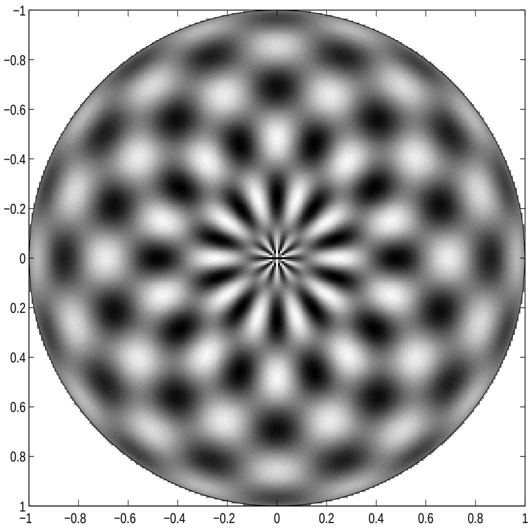

Fig. 7. The modified Chebyshev-function $\widehat{\mathcal{V}}_{6,10}$ resulting from the argument-transform shown in Figure 8 being applied to the Chebyshev-function $\mathcal{V}_{6,10}$

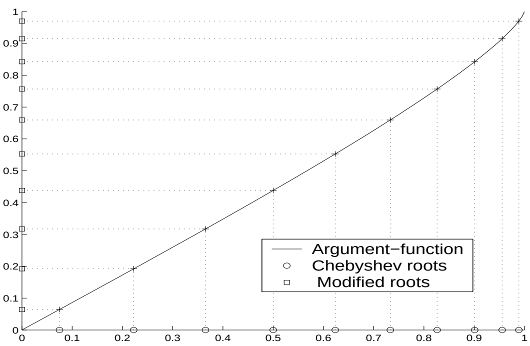

Fig. 8. The argument-function for a circular section (a=1.4) shaped weight function

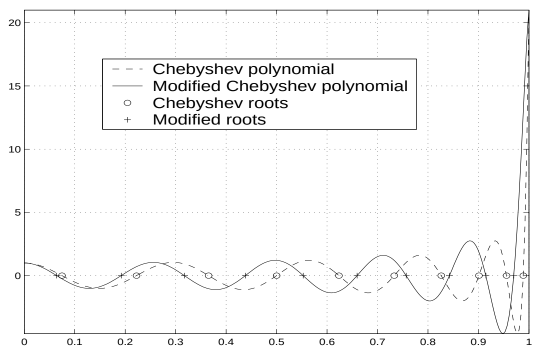

Fig. 9. The Chebyshev-polynomial V_6 modified according to the argument-function shown in Fig. 8

at the function represented in Figure 10), they behave rather "awkwardly" over the origin: they take on a wide range of values near and over the origin. (In the figures, this behaviour is indicated by the crisp star-like artifacts in the centre of the circle.) Such behaviour clearly should be avoided if real cornea surfaces are to be modelled.

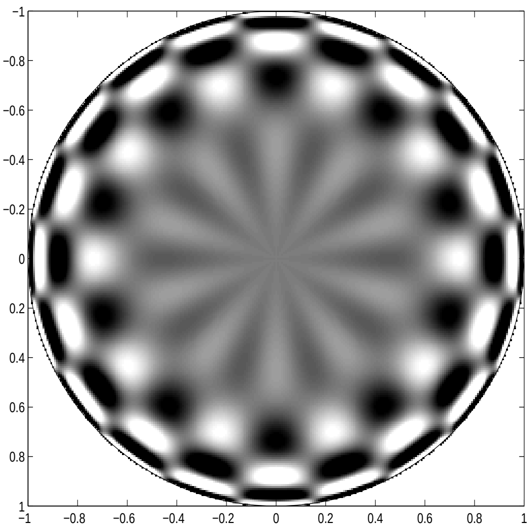

Fig. 10. The modified Chebyshev-function $\breve{\mathcal{V}}_{6,10}$ resulting from the argument-transform shown in Figure 11 being applied to the Chebyshev-function $\mathcal{V}_{6,10}$

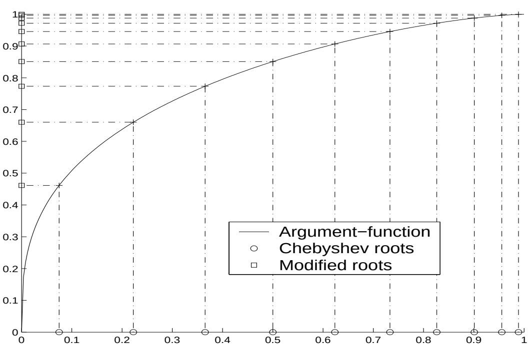

Fig. 11. The argument-function for a weight function that looks like a circular section (a=1.4) turned upside-down

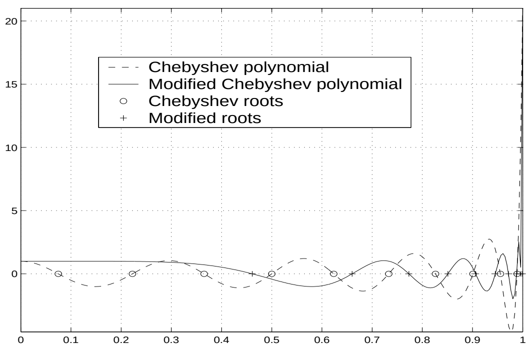

Fig. 12. A Chebyshev-polynomial V_6 modified according to the argument-function shown in Fig. 11

In order to save the useability of the Chebyshev-based system proposed in this paper, elimination of this artifact is necessary e.g. by choosing weighting functions that take 0 at the origin and are smooth and flat enough. One can use, for example, a weighting function ϕ_b that resembles a circular segment turned upside down, that is

$$\varphi_b(r) := a - \sqrt{a^2 - r^2} \qquad (24)$$
$$(0 \le r \le 1, a \ge 1).$$

The use of this weight function in (18) and (19) radically flattens the Chebyshev-polynomials as it is shown in Fig. 12 for V_6. It should be noted that the awkward behaviour over the origin of function $\breve{\mathcal{V}}_{6,10}$ (see Fig. 10) still remains. It is the properly selected weight function (24) that smoothes the elements in the representation series.

5. CONCLUSION AND FUTURE WORK

In this paper, an alternative to the radial Zernike-transformation has been proposed. The proposed orthogonal system of radial functions is based on the Chebyshev-polynomials of the second kind. This system has promising features for representing cornea surfaces, especially, if a properly selected argument transform is applied to its functions. Though, the functions of the original system and its "naïve" modifications exhibit awkward behaviour in the centre of the unit-disc, with a better selection of the weight function - and consequently of the argument transform - produces functions that are applicable to the area of cornea topography. It should be emphasized that further work is required a) in testing the proposed systems capability of representing calotte-like smooth surfaces, b) to derive and check the discrete version of the proposed system and verify its usefulness and precision in representing real cornea surfaces.

REFERENCES

Corbett, M. C., E. S. Rosen and D. P. S. O'Brart (1999). *Corneal Topography: Principles and Applications*. Bmj Publ. Group. London.

Iskander, D. Robert, Mark R. Morelande, Michael J. Collins and Brett Davis (2002). Modeling of corneal surfaces with radial polynomials. *IEEE Trans. on Biomed. Eng.* **49**(11), 320–328.

Iskander, D. Robert, Michael J. Collins and Brett Davis (2001). Optimal modeling of corneal surfaces with Zernike polynomials. *IEEE Trans. on Biomed. Eng.* **48**(11), 87–95.

Németh, J., B. Erdélyi, B. Csákány, P. Gáspár, A. Soumelidis, F. Kahlesz and Zs. Lang (2002). High-speed videotopographic measurement of tear film build-up time. *Inv. Ophthalmology and Vis. Sci.* **43**(6), 1783–1790.

Soumelidis, A., F. Schipp and J. Bokor (2002). Frequency domain representation of signals in rational orthogonal bases. In: *Mediterranean Control Conference*. Lissabon, Portugal.

Szegö, G. (1981). *Orthogonal polynomials*. 4 ed.. AMS. New York.